arXiv:1902.05588v2 [hep-ex] 30 Aug 2019

Observation of $B^0_{(s)} \to J/\psi p\overline{p}$ decays and precision measurements of the $B^0_{(s)}$ masses

LHCb collaboration†

Abstract

The first observation of the decays $B^0_{(s)} \to J/\psi p\overline{p}$ is reported, using proton-proton collision data corresponding to an integrated luminosity of $5.2\,\text{fb}^{-1}$, collected with the LHCb detector. These decays are suppressed due to limited available phase space, as well as due to Okubo-Zweig-Iizuka or Cabibbo suppression. The measured branching fractions are

$$\mathcal{B}(B^0 \to J/\psi p\overline{p}) = (4.51 \pm 0.40\,(\text{stat}) \pm 0.44\,(\text{syst})) \times 10^{-7},$$
$$\mathcal{B}(B^0_s \to J/\psi p\overline{p}) = (3.58 \pm 0.19\,(\text{stat}) \pm 0.39\,(\text{syst})) \times 10^{-6}.$$

For the B^0_s meson, the result is much higher than the expected value of $\mathcal{O}(10^{-9})$. The small available phase space in these decays also allows for the most precise single measurement of both the B^0 mass as $5279.74 \pm 0.30\,(\text{stat}) \pm 0.10\,(\text{syst})\,\text{MeV}$, and the B^0_s mass as $5366.85 \pm 0.19\,(\text{stat}) \pm 0.13\,(\text{syst})\,\text{MeV}$.

---

†Authors are listed at the end of this paper.

Multiquark hadronic states beyond the well-studied quark-antiquark (meson) and three-quark (baryon) combinations remain elusive even sixty years after their prediction in the quark model [1, 2]. Employing an amplitude analysis of $\Lambda_b^0 \to J/\psi p K^-$ decays, the LHCb collaboration has found states consistent with $|uudc\bar{c}\rangle$ pentaquarks decaying to $J/\psi p$ [3,4] (charge conjugation is implied throughout this Letter). The decays $B_{(s)}^0 \to J/\psi p \bar{p}$ are sensitive to pentaquark searches in the $J/\psi p$ and $J/\psi \bar{p}$ components and to glueball states [5,6] in the $p\bar{p}$ system. Baryonic $B_{(s)}^0$ decays are also interesting to study the dynamics of the final baryon-antibaryon system and its characteristic threshold enhancement, whose underlying origin has still to be completely understood [7].

In the leading Feynman diagrams shown in Fig. 1, the B^0 mode is Cabibbo suppressed due to the presence of the Cabibbo-Kobayashi-Maskawa element V_{cd}, while the B_s^0 mode is Okubo-Zweig-Iizuka suppressed [2, 8, 9]. The naïve theoretical expectation for the branching fraction $\mathcal{B}(B_s^0 \to J/\psi p \bar{p})$ is at the level of 10^{-9} [10]. However, the presence of an intermediate pentaquark or glueball state can enhance the decay rate. The authors of Ref. [10] pointed out the potential sensitivity of $B_s^0 \to J/\psi p \bar{p}$ decays to tensor glueball states via a possible resonant contribution of $f_J(2220) \to p\bar{p}$, which could enhance the $B_s^0 \to J/\psi p \bar{p}$ decay branching fraction up to order 10^{-6}. Hints towards such enhancements were noted in a previous LHCb measurement using $1\,\mathrm{fb}^{-1}$ of pp collision data, where no observation for either mode was made, but a 2.8 standard deviation excess was seen for the $B_s^0 \to J/\psi p \bar{p}$ decay [11].

These decays also allow for high-precision mass measurements. The kinetic energies in the $B_{(s)}^0$ rest systems of the decay products (Q-values) are approximately $306\,\mathrm{MeV}$ for B^0 and $393\,\mathrm{MeV}$ for B_s^0 decays. The small Q-values imply a very small contribution from momentum uncertainties to the $B_{(s)}^0$ mass measurements.

In this Letter, the first observation of these modes along with their branching fraction and B^0 and B_s^0 mass measurements are reported employing a data sample corresponding to $5.2\,\mathrm{fb}^{-1}$ of pp collision data collected by the LHCb experiment. As a normalization mode, the copious $B_s^0 \to J/\psi \phi(\to K^+ K^-)$ sample is used, which is similar in topology to the signal channels.

The LHCb detector [12, 13] is a single-arm forward spectrometer covering the
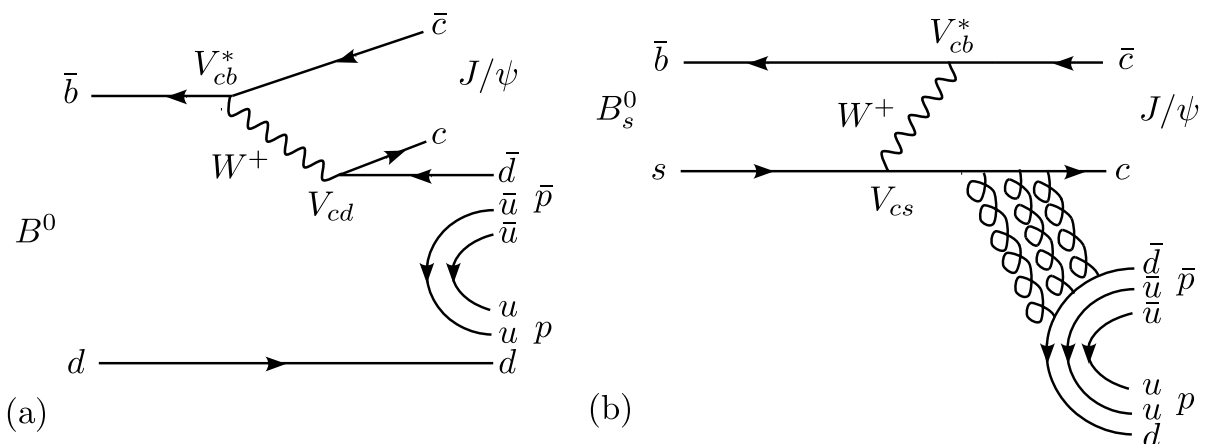

Figure 1: Leading Feynman diagrams for (a) $B^0 \to J/\psi p \bar{p}$ and (b) $B_s^0 \to J/\psi p \bar{p}$ decays.

1

pseudorapidity range $2 < \eta < 5$, designed for the study of particles containing b or c quarks. The detector includes a high-precision tracking system consisting of a silicon-strip vertex detector surrounding the pp interaction region [14], a large-area silicon-strip detector located upstream of a dipole magnet with a bending power of about $4\,\mathrm{Tm}$, and three stations of silicon-strip detectors and straw drift tubes [15] placed downstream of the magnet. The tracking system provides a measurement of the momentum, p, of charged particles with a relative uncertainty that varies from 0.5% at low momentum to 1.0% at $200\,\mathrm{GeV}$.[1] Different types of charged hadrons are distinguished using information from two ring-imaging Cherenkov detectors [16]. Muons are identified by a system composed of alternating layers of iron and multiwire proportional chambers [17]. The online event selection is performed by a trigger [18], comprising a hardware stage based on information from the muon system, followed by a software stage that applies a full event reconstruction. The software trigger is a combination of event categories mostly relying on identifying J/ψ decays consistent with a B-meson decay topology with two muon tracks originating from a secondary decay vertex detached from the primary pp collision point.

The pp collision data used in this analysis were collected at center-of-mass energies of 7 and $8\,\mathrm{TeV}$ ($3\,\mathrm{fb}^{-1}$) and $13\,\mathrm{TeV}$ ($2.2\,\mathrm{fb}^{-1}$), during the Run 1 (2011 and 2012) and Run 2 (2015 and 2016) run periods, respectively. The data taking conditions differ enough between the two run periods, such that they are analyzed separately and the results combined at the end.

Samples of simulated events are used to study the properties of the signal and control channels. The pp collisions are generated using PYTHIA [19] with a specific LHCb configuration [20]. Decays of hadronic particles are described by EVTGEN [21], in which final-state radiation is generated using PHOTOS [22]. For the $B_s^0 \to J/\psi\,\phi$ mode, simulation samples are generated according to a decay model based on results reported in Ref. [23], while the $B_{(s)}^0 \to J/\psi\,p\bar{p}$ signal modes are generated uniformly in phase space. The interactions of the generated particles with the detector and its response are implemented using the GEANT4 toolkit [24] as described in Ref. [25].

The event selection relies on the excellent vertexing and charged particle identification (PID) capabilities of the LHCb detector. For a given particle, the associated primary vertex (PV) corresponds to that with the smallest χ_{IP}^2, defined as the difference in χ^2 between the PV fit including and excluding the particle. Signal candidates are formed starting with a pair of charged tracks, consistent with muons originating from a common vertex significantly displaced from its associated PV and with an invariant mass consistent with the J/ψ meson. Another pair of oppositely charged tracks, identified as protons and originating from a common vertex, is combined with the J/ψ candidate to form a $B_{(s)}^0$ candidate. The entire decay topology is submitted to a kinematic fit where the dimuon invariant mass is constrained to the known J/ψ mass [26]. The $B_s^0 \to J/\psi\,\phi$ control mode candidates are reconstructed in a similar fashion, replacing the $p\bar{p}$ combination with a pair of charged tracks identified as K^+K^- candidates, required to have an invariant mass within $\pm 5\,\mathrm{MeV}$ of the known ϕ-meson mass [26]. All charged tracks are required to be of good quality and have $p_{\mathrm{T}} > 300$ MeV ($p_{\mathrm{T}} > 550$ MeV) for p or K (μ). For the $B_s^0 \to J/\psi\,\phi$ mode, the contamination from $B^0 \to J/\psi\,K^+\pi^-$ decays with a pion misidentified as a kaon is rejected by imposing a B^0 mass veto and using PID information. At this stage, the combinatorial background dominates, comprising a correctly reconstructed J/ψ meson

_____
[1]Natural units with $\hbar = c = 1$ are used throughout.

candidate combined with two unrelated charged tracks.

At this stage, a multidimensional gradient-boosting algorithm [27] is used to weight the simulated $B_s^0 \to J/\psi \phi$ events to match background-subtracted data distributions in all the training variables. These weights are denoted as GB-weights. The background-subtracted data distributions are obtained using the *sPlot* technique [28]. Under the assumption that the relative corrections between data and simulation are similar among different $B_{(s)}^0 \to J/\psi h^+ h'^-$ decay topologies, h^+ and h'^- being charged hadrons, the GB-weights obtained from the control mode are applied to the signal mode. To validate this assumption, similar GB-weights are derived using another control mode, $B^0 \to J/\psi K^+ \pi^-$, yielding similar results.

For further background suppression, two multivariate classifiers are applied, each employing a gradient-boosted decision tree (BDT) [29]. In the first stage, the $\mathrm{BDT_{kin}}$ classifier, based on kinematical and topological variables of the B_s^0 candidate, is trained using the $B_s^0 \to J/\psi \phi$ decays from simulation as signal proxy, and selected $J/\psi K^+ K^-$ candidates in the mass window $[5450, 5700]$ MeV as background. For $\mathrm{BDT_{kin}}$, only kinematic variables whose distributions are similar between the signal and the control mode are employed. These include the p, p_T, and χ^2_{IP} values of the B_s^0 meson, the χ^2 probability from a kinematic fit [30] to the decay topology, and the impact parameter (IP) of the muons with respect to the associated PV.

To choose the $\mathrm{BDT_{kin}}$ selection cut, the $B_s^0 \to J/\psi p\bar{p}$ signal figure of merit, $S/\sqrt{S+B}$, is required to exceed five in a 2σ window around the B_s^0 mass peak. The background yield, B, is estimated from a fit to the $J/\psi p\bar{p}$ invariant mass distribution. To estimate the expected signal yield, S, the central value of the $B_s^0 \to J/\psi p\bar{p}$ branching fraction quoted in Ref. [11] is used, along with the signal efficiency obtained from simulation.

In the final selection stage, a second classifier, $\mathrm{BDT_{PID}}$, uses the hadron PID information from the Cherenkov detector system to distinguish between pions, kaons and protons. Aside from PID, the $\mathrm{BDT_{PID}}$ training variables also include the p, p_T and χ^2_{IP} values of the protons. The signal sample is taken as the $B_s^0 \to J/\psi p\bar{p}$ simulation incorporating the GB-weights for the kinematic variables, while the background sample is taken from events in data with $m(J/\psi p\bar{p}) \in [5450, 5500]$ MeV. The hadron PID variables in the simulation require further corrections to be representative of data. The PID variables are obtained from high-yield calibration samples of $\Lambda_c^+ \to p K^- \pi^+$ and $D^{*+} \to D^0(\to K^- \pi^+)\pi^+$ decays, which can be selected as a function of the p, p_T and the number of tracks in the event using only kinematic information [31]. The optimal $\mathrm{BDT_{PID}}$ selection criterion is chosen by maximizing the figure of merit $S/\sqrt{S+B}$, with the initial signal and background yields obtained from a fit to the $m(J/\psi p\bar{p})$ distribution after the $\mathrm{BDT_{kin}}$ selection.

For the $B_s^0 \to J/\psi \phi$ control mode, the selection is performed using a dedicated classifier, $\mathrm{BDT_{CS}}$, which includes the kinematic variables considered in $\mathrm{BDT_{kin}}$ with the addition of the PID information.

After application of all selection requirements, the background is predominantly combinatorial. Approximately 1% of the selected events contain more than one candidate at this stage; a single candidate is selected randomly. The efficiency of the trigger, detector acceptance, reconstruction and selection procedure is approximately 1%, as estimated from simulation.

The B^0 and B_s^0 signal and background yields are determined via an extended maximum likelihood fit to the $J/\psi p\bar{p}$ invariant mass distribution in the range $[5220, 5420]$ MeV. Each signal shape is modeled as the sum of two Crystal Ball [32] functions sharing a
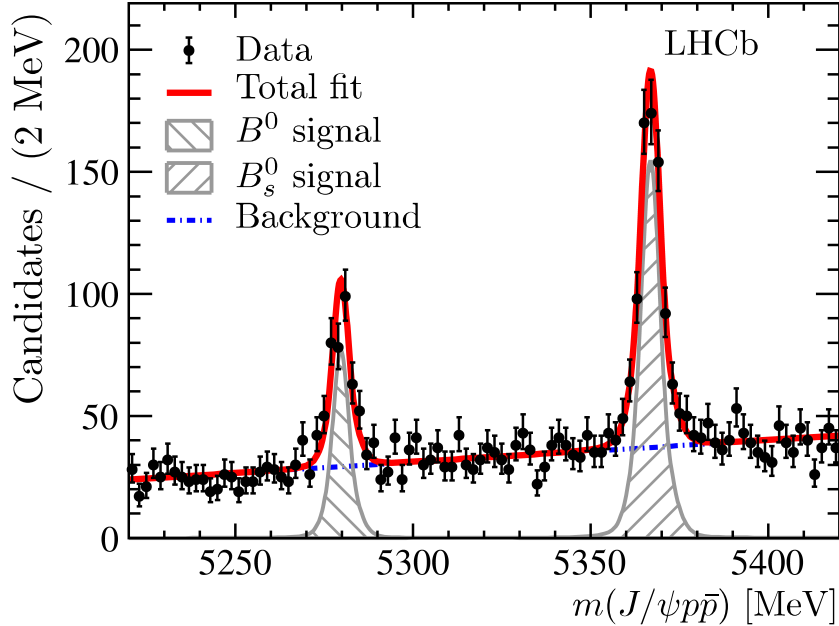
Figure 2: Fit to the $J/\psi\,p\bar{p}$ invariant-mass distribution of the $B^0_{(s)}$ signal modes.

Table 1: Signal yields and masses for B^0 and B^0_s mesons.

Mode	Yield	$B^0_{(s)}$ mass [MeV]
$B^0 \to J/\psi\,p\bar{p}$	256 ± 22	5279.74 ± 0.30
$B^0_s \to J/\psi\,p\bar{p}$	609 ± 31	5366.85 ± 0.19

common peak position, with tails on either sides of the peak to describe the radiative and misreconstruction effects. The background shape is modeled by a first-order polynomial with parameters determined from the fit to data. The signal-model parameters are determined from simulation and only the B^0 and B^0_s central mass values are left as free parameters in the fit to data. The detector invariant-mass resolution is in agreement with simulations within a factor of 1.007 ± 0.004 as determined with the control mode. Residual discrepancies are accounted for in the systematic uncertainties. In order to validate the fit model, 1000 mass spectra are generated according to the model and fitted employing an alternative model comprising three Gaussian components for the signal and an exponential function for background. The difference between the input value of the yields and the mean of the fitted yields from the alternative model is assigned as a systematic uncertainty. The mass fit for the control mode uses a similar B^0_s signal lineshape, with the background modeled by an exponential function. The result of the fit to the combined Run 1 and Run 2 control mode yields a signal of $136,800 \pm 400$. The corresponding fit to the signal-mode candidates is shown in Fig. 2 with the results reported in Table 1, where clear signals of B^0 and B^0_s are observed.

The branching fractions measured with respect to the $B_s^0 \to J/\psi\,\phi$ control mode are

$$\frac{\mathcal{B}(B^0 \to J/\psi\,p\bar{p})}{\mathcal{B}(B_s^0 \to J/\psi\,\phi) \times \mathcal{B}(\phi \to K^+K^-) \times f_s/f_d} = \frac{N_{B^0 \to J/\psi\,p\bar{p}}^{\mathrm{corr}}}{N_{B_s^0 \to J/\psi\,K^+K^-}^{\mathrm{corr}}},$$

$$\frac{\mathcal{B}(B_s^0 \to J/\psi\,p\bar{p})}{\mathcal{B}(B_s^0 \to J/\psi\,\phi) \times \mathcal{B}(\phi \to K^+K^-)} = \frac{N_{B_s^0 \to J/\psi\,p\bar{p}}^{\mathrm{corr}}}{N_{B_s^0 \to J/\psi\,K^+K^-}^{\mathrm{corr}}},$$

where f_s/f_d is the ratio of the b-quark hadronization probabilities into B_s^0 and B^0 mesons, and N^{corr} denotes efficiency-corrected signal yields. For the signal modes, since the physics model is not known *a priori*, an event-by-event efficiency correction is applied to the data. It is derived from simulation as a function of the kinematic variables, which are given in detail in the Appendix.

Since the control mode has a topology very similar to that of the signal mode, most of the systematic uncertainties cancel in the branching-fraction ratio measurement. Residual systematic effects of the PID efficiency estimation are due to the correction procedure. An alternative PID correction is considered using proton calibration samples from decays of the long-lived Λ baryon to a proton and a pion, instead of prompt Λ_c^+ decays. The difference between the two methods is assigned as a systematic uncertainty. The degree to which the simulation describes hadronic interactions with the detector material is less accurate for baryons than it is for mesons [21]. Following Ref. [33], a systematic uncertainty of 4% (1.1%) per proton (kaon) is assigned. Other systematic effects include the choice of the fit model, the weighting procedure, the trigger efficiency, and the presence of events with more than one candidate. The overall systematic uncertainties on the ratio of branching fractions are 7.2% (7.2%) and 6.5% (6.6%) for B_s^0 (B^0) meson in Run 1 and Run 2, respectively, where the relevant contributions, listed in Table 2, are added in quadrature. Since the detector and the analysis methods remain the same between the two run periods, the systematic uncertainties are fully correlated while the statistical uncertainties are uncorrelated. The combination of the measurements is taken as a weighted mean to give the branching fraction ratios

$$\frac{\mathcal{B}(B^0 \to J/\psi\,p\bar{p})}{\mathcal{B}(B_s^0 \to J/\psi\,\phi) \times \mathcal{B}(\phi \to K^+K^-) \times f_s/f_d} = (0.329 \pm 0.029\,(\mathrm{stat}) \pm 0.022\,(\mathrm{syst})) \times 10^{-2},$$

$$\frac{\mathcal{B}(B_s^0 \to J/\psi\,p\bar{p})}{\mathcal{B}(B_s^0 \to J/\psi\,\phi) \times \mathcal{B}(\phi \to K^+K^-)} = (0.706 \pm 0.037\,(\mathrm{stat}) \pm 0.048\,(\mathrm{syst})) \times 10^{-2},$$

where the first uncertainty is statistical and the second is systematic. For the absolute branching-fraction determination, the value $\mathcal{B}(B_s^0 \to J/\psi\,\phi) \times \mathcal{B}(\phi \to K^+K^-) \times f_s/f_d = (1.314 \pm 0.016 \pm 0.079) \times 10^{-4}$ is obtained from Ref. [34] as the product of the two branching ratios, $\mathcal{B}(B_s^0 \to J/\psi\,\phi) = (10.50 \pm 0.13 \pm 0.64) \times 10^{-4}$ and $\mathcal{B}(\phi \to K^+K^-) = 0.489 \pm 0.005$, and the ratio of fragmentation probabilities $f_s/f_d = 0.256 \pm 0.020$ [35]. For the B_s^0-meson normalization, the updated ratio $f_s/f_d = 0.259 \pm 0.015$ [35] is used in Run 1, while for Run 2 it has been multiplied by an additional scale factor of 1.068 ± 0.046 [36] to take into account the dependence on the center of mass energy. The small S-wave K^+K^- fraction under the $\phi(1020)$ resonance, $F_S = 0.0070 \pm 0.0005$ [34], is accounted for as a correction. The absolute branching fractions are then combined to give

$$\mathcal{B}(B^0 \to J/\psi\,p\bar{p}) = (4.51 \pm 0.40\,(\mathrm{stat}) \pm 0.44\,(\mathrm{syst})) \times 10^{-7},$$

$$\mathcal{B}(B_s^0 \to J/\psi\,p\bar{p}) = (3.58 \pm 0.19\,(\mathrm{stat}) \pm 0.39\,(\mathrm{syst})) \times 10^{-6},$$

Table 2: Systematic uncertainties on the branching fraction measurements for Run 1 and Run 2. The total uncertainties on the branching fraction ratios (BFR) are the sum of the systematic uncertainties, added in quadrature. The total uncertainties on the absolute branching fractions ($\mathcal{B}$) include the normalization and the uncertainties on the ratio f_s/f_d from external measurments as well.

	$\mathcal{B}(B^0 \to J/\psi\, p\bar{p})$	$\mathcal{B}(B_s^0 \to J/\psi\, p\bar{p})$
	Run 1 (Run 2)	Run 1 (Run 2)
Fit model	1.0 (0.5)%	1.0 (0.9)%
Detector resolution	0.6 (0.5)%	0.4 (0.6)%
PID efficiency	5.0 (4.0)%	5.0 (4.0)%
Trigger	1.0 (1.0)%	1.0 (1.0)%
Tracking	5.0 (5.0)%	5.0 (5.0)%
Simulation weighting	0.4 (0.4)%	0.3 (0.3)%
Multiple candidates	0.1 (0.1)%	0.1 (0.1)%
Total on BFR	7.2 (6.5)%	7.2 (6.6)%
Normalization	6.1 (6.1)%	6.1 (6.1)%
f_s/f_d	$-$ (4.3)%	5.8 (5.8)%
Total on $\mathcal{B}$	9.4 (10.1)%	11.1 (10.7)%

where the systematic uncertainty is the sum in quadrature of the overall systematic contribution on the ratio of branching fractions, the normalization mode uncertainty and the f_s/f_d uncertainty for the B_s^0 signal. Table 2 summarizes the systematic uncertainties separately for the run periods. The dominant contributions are the normalization, the PID, and the tracking systematic uncertainties. For the B^0 meson, the external normalization measurement from Run 1, $\mathcal{B}(B_s^0 \to J/\psi\,\phi) \times \mathcal{B}(\phi \to K^+K^-) \times f_s/f_d$ [34] is used, while for Run 2 the additional energy-dependent correction on f_s/f_d has an uncertainty of 4.3%. For the B_s^0 meson, the measured $\mathcal{B}(B_s^0 \to J/\psi\,\phi) \times \mathcal{B}(\phi \to K^+K^-) \times f_s/f_d$ is divided by f_s/f_d to obtain the B_s^0 normalization, $\mathcal{B}(B_s^0 \to J/\psi\,\phi) \times \mathcal{B}(\phi \to K^+K^-)$, resulting in an uncertainty on f_s/f_d independent of the run condition.

In addition, the small Q-values of the $B_{(s)}^0 \to J/\psi\, p\bar{p}$ decays also allow for precise measurements of the B^0 and B_s^0 masses, with a resolution of 3.3 MeV (3.8 MeV) for the B^0 (B_s^0) meson. The sources of systematic uncertainties include momentum scaling due to imperfections in the magnetic-field mapping derived using well-known narrow resonances, uncertainties on particle interactions with the detector material, and the choice of the

Table 3: Systematic uncertainties of B^0 and B_s^0 mass measurements.

	B^0	B_s^0
	[MeV]	[MeV]
Momentum scale	0.097	0.124
Mass fit model	0.020	0.020
Energy loss correction	0.030	0.030
Total	0.103	0.129

signal model, as reported in Table 3. The uncertainty on the proton mass is neglected. The final results are

$$m_{B^0} = 5279.74 \pm 0.30 \,(\text{stat}) \pm 0.10 \,(\text{syst}) \,\text{MeV},$$
$$m_{B_s^0} = 5366.85 \pm 0.19 \,(\text{stat}) \pm 0.13 \,(\text{syst}) \,\text{MeV},$$

with a correlation of 4×10^{-4} in the statistical uncertainty. These represent the most precise single measurements for the B^0 and B_s^0 masses.

In summary, the first observation of the $B^0 \to J/\psi \, p\bar{p}$ and $B_s^0 \to J/\psi \, p\bar{p}$ decays is reported. The measured branching fraction for the $B^0 \to J/\psi \, p\bar{p}$ decay is consistent with theoretical expectations [10] while that for $B_s^0 \to J/\psi \, p\bar{p}$ is enhanced by two orders of magnitude with respect to predictions without resonant contributions [10]. More data are needed for glueball and pentaquark searches through a full Dalitz plot analysis. The world's best single measurements of the B^0 and B_s^0 masses are also reported.

Acknowledgements
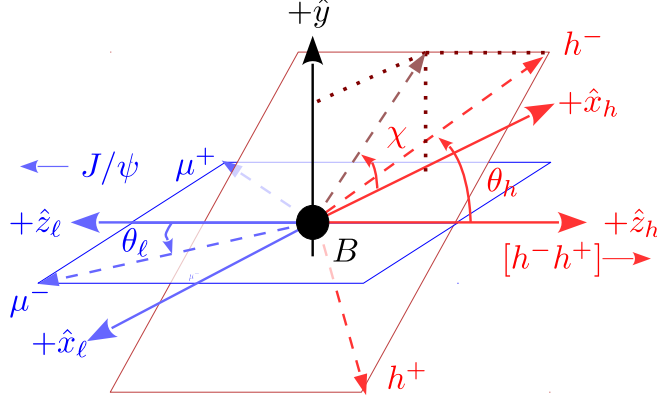
Appendix

A. Efficiency parameterization for the signal mode

Figure 3: The three angular variables $\{\theta_\ell, \theta_h, \chi\}$ for the decay $B \to J/\psi (\to \mu^+\mu^-)h^+h^-$, where $h \in \{p, K\}$. The dihadron (in red) and dilepton (in blue) coordinate systems lie back-to-back with a common vertical $\hat{y}$ axis. The angle between the decay planes is $\chi \in (-\pi, \pi]$, while the two helicity angles, θ_h and θ_ℓ, are defined in the dihadron and dilepton rest frames, respectively.

The 4-body phase-space of the decay $B \to J/\psi (\to \mu^+\mu^-)h^+h^-$, where $h \in \{p, K\}$, is fully described by four independent kinematic variables. One of them is the dihadron invariant mass $m_{h^+h^-}$. For a given $m_{h^+h^-}$, the topology can be described by three angles, shown in Fig. 3:

- θ_ℓ and θ_h: the helicity angles defined in the dimuon and dihadron rest frames, respectively;

- χ: the azimuthal angle between the two decay planes of the dilepton and dihadron systems.

Since the final state is self-conjugate, the h^- and the μ^- particles are chosen to define the angles, for both $B^0_{(s)}$ and $\overline{B}^0_{(s)}$ mesons. For the signal mode, the overall efficiency, including trigger, detector acceptance and selection procedure, is obtained from simulation as a function of the four kinematic variables, $\vec{\varphi} \equiv \{m'_{p\bar{p}}, \cos\theta_\ell, \cos\theta_h, \chi'\}$. Here, $m'_{p\bar{p}}$ and χ' are normalized such that all four variables in $\vec{\varphi}$ lie in the range $(-1, 1]$. The efficiency is parameterized as the product of Legendre polynomials

$$\varepsilon(\vec{\varphi}) = \sum_{i,j,k,l} c_{i,j,k,l} \; P(\cos\theta_\ell, i)P(\cos\theta_h, j)P(\chi', k)P(m'_{p\bar{p}}, l),$$

where $P(x, n)$ is a Legendre polynomial of order n in $x \in (-1, 1]$. Employing the maximum order of the polynomials as $\{3, 7, 7, 5\}$ for $\{m'_{p\bar{p}}, \cos\theta_\ell, \cos\theta_h, \chi'\}$, respectively, was found to give a good parameterization. Simulation samples are employed, where $B^0_{(s)} \to J/\psi \, p\bar{p}$ events are generated uniformly in phase space. The coefficients, $c_{i,j,k,l}$, are determined

from the simulation using a moments technique employing the orthogonality of Legendre polynomials

$$c_{i,j,k,l} = C \sum_{n=0}^{N_{\text{recon}}} \left(\frac{2i+1}{2}\right)\left(\frac{2j+1}{2}\right)\left(\frac{2k+1}{2}\right)\left(\frac{2l+1}{2}\right)$$
$$\times P(\cos\theta_\ell, i)P(\cos\theta_h, j)P(\chi', k)P(m'_{p\bar{p}}, l).$$

The sum is over the number of reconstructed decays, N_{recon}, in the simulation sample after all selection criteria. The prefactor C ensures appropriate normalization. For a given data candidate, the corresponding kinematic variables, $\vec{\varphi}$, are reconstructed and the efficiency, $\varepsilon(\vec{\varphi})$, is computed according to the parameterization. The candidate is subsequently assigned a weight, $1/\varepsilon(\vec{\varphi})$, to account for the detector efficiency.

B. Combining the Run 1 and Run 2 branching fraction results

The ratio of branching fractions for Run 1 and Run 2 are provided here separately. For Run 1,

$$\frac{\mathcal{B}(B^0 \to J/\psi\, p\bar{p})}{\mathcal{B}(B_s^0 \to J/\psi\,\phi) \times \mathcal{B}(\phi \to K^+K^-) \times f_s/f_d} = (0.35 \pm 0.05(\text{stat}) \pm 0.02(\text{syst})) \times 10^{-2},$$

$$\frac{\mathcal{B}(B_s^0 \to J/\psi\, p\bar{p})}{\mathcal{B}(B_s^0 \to J/\psi\,\phi) \times \mathcal{B}(\phi \to K^+K^-)} = (0.68 \pm 0.06(\text{stat}) \pm 0.05(\text{syst})) \times 10^{-2},$$

while for Run 2,

$$\frac{\mathcal{B}(B^0 \to J/\psi\, p\bar{p})}{\mathcal{B}(B_s^0 \to J/\psi\,\phi) \times \mathcal{B}(\phi \to K^+K^-) \times f_s/f_d} = (0.32 \pm 0.04(\text{stat}) \pm 0.02(\text{syst})) \times 10^{-2}.$$

$$\frac{\mathcal{B}(B_s^0 \to J/\psi\, p\bar{p})}{\mathcal{B}(B_s^0 \to J/\psi\,\phi) \times \mathcal{B}(\phi \to K^+K^-)} = (0.72 \pm 0.05(\text{stat}) \pm 0.05(\text{syst})) \times 10^{-2}.$$

The absolute branching fractions obtained from our present knowledge of $\mathcal{B}(B_s^0 \to J/\psi\,\phi) \times \mathcal{B}(\phi \to K^+K^-) \times f_s/f_d = (1.314 \pm 0.016 \pm 0.079) \times 10^{-4}$ and $f_s/f_d = 0.259 \pm 0.015$ are, for Run 1,

$$\mathcal{B}(B^0 \to J/\psi\, p\bar{p}) = (4.54 \pm 0.62(\text{stat}) \pm 0.33(\text{syst}) \pm 0.28(\text{norm})) \times 10^{-7},$$
$$\mathcal{B}(B_s^0 \to J/\psi\, p\bar{p}) = (3.45 \pm 0.31(\text{stat}) \pm 0.25(\text{syst}) \pm 0.21(\text{norm}) \pm 0.20(f_s/f_d)) \times 10^{-6},$$

and for Run 2,

$$\mathcal{B}(B^0 \to J/\psi\, p\bar{p}) = (4.49 \pm 0.52(\text{stat}) \pm 0.29(\text{syst}) \pm 0.28(\text{norm}) \pm 0.19(f_s/f_d)) \times 10^{-7},$$
$$\mathcal{B}(B_s^0 \to J/\psi\, p\bar{p}) = (3.66 \pm 0.25(\text{stat}) \pm 0.24(\text{syst}) \pm 0.22(\text{norm}) \pm 0.21(f_s/f_d)) \times 10^{-6}.$$

To combine the results from the Run 1 and Run 2 data samples, the systematic uncertainties are taken as fully correlated between the run periods, since the data are collected employing the same detector and analysis techniques. The statistical uncertainties are considered uncorrelated since the datasets are disjoint. The covariance matrices are constructed as

$$V = \begin{pmatrix} \sigma^2_{\text{stat, Run 1}} + \sigma^2_{\text{syst, Run 1}} & \sigma_{\text{syst, Run 1}} \times \sigma_{\text{syst, Run 2}} \\ \sigma_{\text{syst, Run 1}} \times \sigma_{\text{syst, Run 2}} & \sigma^2_{\text{stat, Run 2}} + \sigma^2_{\text{syst, Run 2}} \end{pmatrix},$$

with the numerical values for the absolute branching fraction combination as

$$V_{B^0} = \begin{pmatrix} 0.5667 & 0.1916 \\ 0.1916 & 0.4722 \end{pmatrix} \times 10^{-14},$$

$$V_{B_s^0} = \begin{pmatrix} 0.2401 & 0.1502 \\ 0.1502 & 0.2142 \end{pmatrix} \times 10^{-12}.$$

The weighted mean value and uncertainty are then calculated as

$$\overline{x} = \sum_{i \in \{1,2\}} w_i x_i,$$

$$\sigma_x^2 = \sum_{i,k \in \{1,2\}} w_i w_k V_{ik},$$

respectively, where the variable x denotes the branching fraction and the weights are obtained from the inverse of the aforementioned covariance matrix as

$$w_i = \frac{\sum\limits_{k \in \{1,2\}} (V^{-1})_{ik}}{\sum\limits_{j,k \in \{1,2\}} (V^{-1})_{jk}}.$$

References

[1] M. Gell-Mann, *A schematic model of baryons and mesons*, Phys. Lett. **8** (1964) 214.

[2] G. Zweig, *An SU_3 model for strong interaction symmetry and its breaking*, Tech. Rep. CERN-TH-401, CERN, Geneva, Jan. 1964.

[3] LHCb collaboration, R. Aaij *et al.*, *Observation of $J/\psi p$ resonances consistent with pentaquark states in $\Lambda_b^0 \to J/\psi pK^-$ decays*, Phys. Rev. Lett. **115** (2015) 072001, arXiv:1507.03414.

[4] LHCb collaboration, R. Aaij *et al.*, *Model-independent evidence for $J/\psi p$ contributions to $\Lambda_b^0 \to J/\psi pK^-$ decays*, Phys. Rev. Lett. **117** (2016) 082002, arXiv:1604.05708.

[5] C. J. Morningstar and M. Peardon, *Glueball spectrum from an anisotropic lattice study*, Phys. Rev. **D60** (1999) 034509, arXiv:hep-lat/9901004.

[6] Y. Chen *et al.*, *Glueball spectrum and matrix elements on anisotropic lattices*, Phys. Rev. **D73** (2006) 014516, arXiv:hep-lat/0510074.

[7] J. L. Rosner, *Low-mass baryon-antibaryon enhancements in B decays*, Phys. Rev. **D68** (2003) 014004, arXiv:hep-ph/0303079.

[8] S. Okubo, *φ-meson and unitary symmetry model*, Phys. Lett. **5** (1963) 165.

[9] J. Iizuka, *A systematics and phenomenology of meson family*, Prog. Theor. Phys. Suppl. **37** (1966) 21.

[10] Y. K. Hsiao and C. Q. Geng, $f_J(2220)$ *and hadronic* $\bar{B}_s^0$ *decays*, Eur. Phys. J. **C75** (2015) 101, arXiv:1412.4900.

[11] LHCb collaboration, R. Aaij *et al.*, *Searches for* $B_{(s)}^0 \to J/\psi\, p\bar{p}$ *and* $B^+ \to J/\psi\, p\bar{p}\pi^+$ *decays*, JHEP **09** (2013) 006, arXiv:1306.4489.

[12] LHCb collaboration, A. A. Alves Jr. *et al.*, *The LHCb detector at the LHC*, JINST **3** (2008) S08005.

[13] LHCb collaboration, R. Aaij *et al.*, *LHCb detector performance*, Int. J. Mod. Phys. **A30** (2015) 1530022, arXiv:1412.6352.

[14] R. Aaij *et al.*, *Performance of the LHCb Vertex Locator*, JINST **9** (2014) P09007, arXiv:1405.7808.

[15] R. Arink *et al.*, *Performance of the LHCb Outer Tracker*, JINST **9** (2014) P01002, arXiv:1311.3893.

[16] M. Adinolfi *et al.*, *Performance of the LHCb RICH detector at the LHC*, Eur. Phys. J. **C73** (2013) 2431, arXiv:1211.6759.

[17] A. A. Alves Jr. *et al.*, *Performance of the LHCb muon system*, JINST **8** (2013) P02022, arXiv:1211.1346.

[18] R. Aaij *et al.*, *The LHCb trigger and its performance in 2011*, JINST **8** (2013) P04022, arXiv:1211.3055.

[19] T. Sjöstrand, S. Mrenna, and P. Skands, *PYTHIA 6.4 physics and manual*, JHEP **05** (2006) 026, arXiv:hep-ph/0603175; T. Sjöstrand, S. Mrenna, and P. Skands, *A brief introduction to PYTHIA 8.1*, Comput. Phys. Commun. **178** (2008) 852, arXiv:0710.3820.

[20] I. Belyaev *et al.*, *Handling of the generation of primary events in Gauss, the LHCb simulation framework*, J. Phys. Conf. Ser. **331** (2011) 032047.

[21] D. J. Lange, *The EvtGen particle decay simulation package*, Nucl. Instrum. Meth. **A462** (2001) 152.

[22] P. Golonka and Z. Was, *PHOTOS Monte Carlo: A precision tool for QED corrections in Z and W decays*, Eur. Phys. J. **C45** (2006) 97, arXiv:hep-ph/0506026.

[23] LHCb collaboration, R. Aaij *et al.*, *Precision measurement of CP violation in* $B_s^0 \to J/\psi\, K^+ K^-$ *decays*, Phys. Rev. Lett. **114** (2015) 041801, arXiv:1411.3104.

[24] Geant4 collaboration, J. Allison *et al.*, *Geant4 developments and applications*, IEEE Trans. Nucl. Sci. **53** (2006) 270; Geant4 collaboration, S. Agostinelli *et al.*, *Geant4: A simulation toolkit*, Nucl. Instrum. Meth. **A506** (2003) 250.

[25] M. Clemencic *et al.*, *The LHCb simulation application, Gauss: Design, evolution and experience*, J. Phys. Conf. Ser. **331** (2011) 032023.

[26] Particle Data Group, M. Tanabashi *et al.*, *Review of particle physics*, Phys. Rev. **D98** (2018) 030001.

[27] A. Rogozhnikov, *Reweighting with Boosted Decision Trees*, J. Phys. Conf. Ser. **762** (2016) 012036, arXiv:1608.05806.

[28] M. Pivk and F. R. Le Diberder, *sPlot: A statistical tool to unfold data distributions*, Nucl. Instrum. Meth. **A555** (2005) 356, arXiv:physics/0402083.

[29] L. Breiman, J. H. Friedman, R. A. Olshen, and C. J. Stone, *Classification and regression trees*, Wadsworth international group, Belmont, California, USA, 1984.

[30] W. D. Hulsbergen, *Decay chain fitting with a Kalman filter*, Nucl. Instrum. Meth. **A552** (2005) 566, arXiv:physics/0503191.

[31] R. Aaij *et al.*, *Selection and processing of calibration samples to measure the particle identification performance of the LHCb experiment in Run 2*, arXiv:1803.00824.

[32] T. Skwarnicki, *A study of the radiative cascade transitions between the Upsilon-prime and Upsilon resonances*, PhD thesis, Institute of Nuclear Physics, Krakow, 1986, DESY-F31-86-02.

[33] LHCb collaboration, R. Aaij *et al.*, *Evidence for the two-body charmless baryonic decay $B^+ \to p\overline{\Lambda}$*, JHEP **04** (2017) 162, arXiv:1611.07805.

[34] LHCb collaboration, R. Aaij *et al.*, *Amplitude analysis and branching fraction measurement of $\overline{B}_s^0 \to J/\psi K^+ K^-$*, Phys. Rev. **D87** (2013) 072004, arXiv:1302.1213.

[35] LHCb collaboration, R. Aaij *et al.*, *Measurement of the fragmentation fraction ratio f_s/f_d and its dependence on B meson kinematics*, JHEP **04** (2013) 001, arXiv:1301.5286, f_s/f_d value updated in LHCb-CONF-2013-011.

[36] LHCb collaboration, R. Aaij *et al.*, *Measurement of the $B_s^0 \to \mu^+\mu^-$ branching fraction and effective lifetime and search for $B^0 \to \mu^+\mu^-$ decays*, Phys. Rev. Lett. **118** (2017) 191801, arXiv:1703.05747.

LHCb Collaboration

R. Aaij[29], C. Abellán Beteta[46], B. Adeva[43], M. Adinolfi[50], C.A. Aidala[77], Z. Ajaltouni[7],
S. Akar[61], P. Albicocco[20], J. Albrecht[12], F. Alessio[44], M. Alexander[55], A. Alfonso Albero[42],
G. Alkhazov[35], P. Alvarez Cartelle[57], A.A. Alves Jr[43], S. Amato[2], S. Amerio[25], Y. Amhis[9],
L. An[19], L. Anderlini[19], G. Andreassi[45], M. Andreotti[18], J.E. Andrews[62], F. Archilli[29],
J. Arnau Romeu[8], A. Artamonov[41], M. Artuso[63], K. Arzymatov[39], E. Aslanides[8], M. Atzeni[46],
B. Audurier[24], S. Bachmann[14], J.J. Back[52], S. Baker[57], V. Balagura[9,b], W. Baldini[18],
A. Baranov[39], R.J. Barlow[58], G.C. Barrand[9], S. Barsuk[9], W. Barter[58], M. Bartolini[21],
F. Baryshnikov[73], V. Batozskaya[33], B. Batsukh[63], A. Battig[12], V. Battista[45], A. Bay[45],
J. Beddow[55], F. Bedeschi[26], I. Bediaga[1], A. Beiter[63], L.J. Bel[29], S. Belin[24], N. Beliy[4],
V. Bellee[45], N. Belloli[22,i], K. Belous[41], I. Belyaev[36], G. Bencivenni[20], E. Ben-Haim[10],
S. Benson[29], S. Beranek[11], A. Berezhnoy[37], R. Bernet[46], D. Berninghoff[14], E. Bertholet[10],
A. Bertolin[25], C. Betancourt[46], F. Betti[17,44], M.O. Bettler[51], Ia. Bezshyiko[46], S. Bhasin[50],
J. Bhom[31], M.S. Bieker[12], S. Bifani[49], P. Billoir[10], A. Birnkraut[12], A. Bizzeti[19,u], M. Bjørn[59],
M.P. Blago[44], T. Blake[52], F. Blanc[45], S. Blusk[63], D. Bobulska[55], V. Bocci[28], O. Boente Garcia[43],
T. Boettcher[60], A. Bondar[40,x], N. Bondar[35], S. Borghi[58,44], M. Borisyak[39], M. Borsato[43],
M. Boubdir[11], T.J.V. Bowcock[56], C. Bozzi[18,44], S. Braun[14], M. Brodski[44], J. Brodzicka[31],
A. Brossa Gonzalo[52], D. Brundu[24,44], E. Buchanan[50], A. Buonaura[46], C. Burr[58], A. Bursche[24],
J. Buytaert[44], W. Byczynski[44], S. Cadeddu[24], H. Cai[67], R. Calabrese[18,g], R. Calladine[49],
M. Calvi[22,i], M. Calvo Gomez[42,m], A. Camboni[42,m], P. Campana[20], D.H. Campora Perez[44],
L. Capriotti[17,e], A. Carbone[17,e], G. Carboni[27], R. Cardinale[21], A. Cardini[24], P. Carniti[22,i],
K. Carvalho Akiba[2], G. Casse[56], M. Cattaneo[44], G. Cavallero[21], R. Cenci[26,p], D. Chamont[9],
M.G. Chapman[50], M. Charles[10], Ph. Charpentier[44], G. Chatzikonstantinidis[49], M. Chefdeville[6],
V. Chekalina[39], C. Chen[3], S. Chen[24], S.-G. Chitic[44], V. Chobanova[43], M. Chrzaszcz[44],
A. Chubykin[35], P. Ciambrone[20], X. Cid Vidal[43], G. Ciezarek[44], F. Cindolo[17], P.E.L. Clarke[54],
M. Clemencic[44], H.V. Cliff[51], J. Closier[44], V. Coco[44], J.A.B. Coelho[9], J. Cogan[8], E. Cogneras[7],
L. Cojocariu[34], P. Collins[44], T. Colombo[44], A. Comerma-Montells[14], A. Contu[24], G. Coombs[44],
S. Coquereau[42], G. Corti[44], M. Corvo[18,g], C.M. Costa Sobral[52], B. Couturier[44], G.A. Cowan[54],
D.C. Craik[60], A. Crocombe[52], M. Cruz Torres[1], R. Currie[54], F. Da Cunha Marinho[2],
C.L. Da Silva[78], E. Dall'Occo[29], J. Dalseno[43,v], C. D'Ambrosio[44], A. Danilina[36], P. d'Argent[14],
A. Davis[58], O. De Aguiar Francisco[44], K. De Bruyn[44], S. De Capua[58], M. De Cian[45],
J.M. De Miranda[1], L. De Paula[2], M. De Serio[16,d], P. De Simone[20], J.A. de Vries[29], C.T. Dean[55],
W. Dean[77], D. Decamp[6], L. Del Buono[10], B. Delaney[51], H.-P. Dembinski[13], M. Demmer[12],
A. Dendek[32], D. Derkach[74], O. Deschamps[7], F. Desse[9], F. Dettori[56], B. Dey[68], A. Di Canto[44],
P. Di Nezza[20], S. Didenko[73], H. Dijkstra[44], F. Dordei[24], M. Dorigo[44,y], A.C. dos Reis[1],
A. Dosil Suárez[43], L. Douglas[55], A. Dovbnya[47], K. Dreimanis[56], L. Dufour[29], G. Dujany[10],
P. Durante[44], J.M. Durham[78], D. Dutta[58], R. Dzhelyadin[41,†], M. Dziewiecki[14], A. Dziurda[31],
A. Dzyuba[35], S. Easo[53], U. Egede[57], V. Egorychev[36], S. Eidelman[40,x], S. Eisenhardt[54],
U. Eitschberger[12], R. Ekelhof[12], L. Eklund[55], S. Ely[63], A. Ene[34], S. Escher[11], S. Esen[29],
T. Evans[61], A. Falabella[17], C. Färber[44], N. Farley[49], S. Farry[56], D. Fazzini[22,44,i], M. Féo[44],
P. Fernandez Declara[44], A. Fernandez Prieto[43], F. Ferrari[17,e], L. Ferreira Lopes[45],
F. Ferreira Rodrigues[2], M. Ferro-Luzzi[44], S. Filippov[38], R.A. Fini[16], M. Fiorini[18,g], M. Firlej[32],
C. Fitzpatrick[45], T. Fiutowski[32], F. Fleuret[9,b], M. Fontana[44], F. Fontanelli[21,h], R. Forty[44],
V. Franco Lima[56], M. Frank[44], C. Frei[44], J. Fu[23,q], W. Funk[44], E. Gabriel[54],
A. Gallas Torreira[43], D. Galli[17,e], S. Gallorini[25], S. Gambetta[54], Y. Gan[3], M. Gandelman[2],
P. Gandini[23], Y. Gao[3], L.M. Garcia Martin[76], J. García Pardiñas[46], B. Garcia Plana[43],
J. Garra Tico[51], L. Garrido[42], D. Gascon[42], C. Gaspar[44], L. Gavardi[12], G. Gazzoni[7],
D. Gerick[14], E. Gersabeck[58], M. Gersabeck[58], T. Gershon[52], D. Gerstel[8], Ph. Ghez[6],
V. Gibson[51], O.G. Girard[45], P. Gironella Gironell[42], L. Giubega[34], K. Gizdov[54],

13

V.V. Gligorov[10], C. Göbel[65], D. Golubkov[36], A. Golutvin[57,73], A. Gomes[1,a], I.V. Gorelov[37],
C. Gotti[22,i], E. Govorkova[29], J.P. Grabowski[14], R. Graciani Diaz[42], L.A. Granado Cardoso[44],
E. Graugés[42], E. Graverini[46], G. Graziani[19], A. Grecu[34], R. Greim[29], P. Griffith[24], L. Grillo[58],
L. Gruber[44], B.R. Gruberg Cazon[59], O. Grünberg[70], C. Gu[3], E. Gushchin[38], A. Guth[11],
Yu. Guz[41,44], T. Gys[44], T. Hadavizadeh[59], C. Hadjivasiliou[7], G. Haefeli[45], C. Haen[44],
S.C. Haines[51], B. Hamilton[62], X. Han[14], T.H. Hancock[59], S. Hansmann-Menzemer[14],
N. Harnew[59], T. Harrison[56], C. Hasse[44], M. Hatch[44], J. He[4], M. Hecker[57], K. Heinicke[12],
A. Heister[12], K. Hennessy[56], L. Henry[76], M. Heß[70], J. Heuel[11], A. Hicheur[64],
R. Hidalgo Charman[58], D. Hill[59], M. Hilton[58], P.H. Hopchev[45], J. Hu[14], W. Hu[68], W. Huang[4],
Z.C. Huard[61], W. Hulsbergen[29], T. Humair[57], M. Hushchyn[74], D. Hutchcroft[56], D. Hynds[29],
P. Ibis[12], M. Idzik[32], P. Ilten[49], A. Inglessi[35], A. Inyakin[41], K. Ivshin[35], R. Jacobsson[44],
J. Jalocha[59], E. Jans[29], B.K. Jashal[76], A. Jawahery[62], F. Jiang[3], M. John[59], D. Johnson[44],
C.R. Jones[51], C. Joram[44], B. Jost[44], N. Jurik[59], S. Kandybei[47], M. Karacson[44], J.M. Kariuki[50],
S. Karodia[55], N. Kazeev[74], M. Kecke[14], F. Keizer[51], M. Kelsey[63], M. Kenzie[51], T. Ketel[30],
E. Khairullin[39], B. Khanji[44], C. Khurewathanakul[45], K.E. Kim[63], T. Kirn[11], V.S. Kirsebom[45],
S. Klaver[20], K. Klimaszewski[33], T. Klimkovich[13], S. Koliiev[48], M. Kolpin[14], R. Kopecna[14],
P. Koppenburg[29], I. Kostiuk[29,48], S. Kotriakhova[35], M. Kozeiha[7], L. Kravchuk[38], M. Kreps[52],
F. Kress[57], P. Krokovny[40,x], W. Krupa[32], W. Krzemien[33], W. Kucewicz[31,l], M. Kucharczyk[31],
V. Kudryavtsev[40,x], A.K. Kuonen[45], T. Kvaratskheliya[36,44], D. Lacarrere[44], G. Lafferty[58],
A. Lai[24], D. Lancierini[46], G. Lanfranchi[20], C. Langenbruch[11], T. Latham[52], C. Lazzeroni[49],
R. Le Gac[8], R. Lefèvre[7], A. Leflat[37], F. Lemaitre[44], O. Leroy[8], T. Lesiak[31], B. Leverington[14],
P.-R. Li[4,ab], Y. Li[5], Z. Li[63], X. Liang[63], T. Likhomanenko[72], R. Lindner[44], F. Lionetto[46],
V. Lisovskyi[9], G. Liu[66], X. Liu[3], D. Loh[52], A. Loi[24], I. Longstaff[55], J.H. Lopes[2], G.H. Lovell[51],
D. Lucchesi[25,o], M. Lucio Martinez[43], Y. Luo[3], A. Lupato[25], E. Luppi[18,g], O. Lupton[44],
A. Lusiani[26], X. Lyu[4], F. Machefert[9], F. Maciuc[34], V. Macko[45], P. Mackowiak[12],
S. Maddrell-Mander[50], O. Maev[35,44], K. Maguire[58], D. Maisuzenko[35], M.W. Majewski[32],
S. Malde[59], B. Malecki[44], A. Malinin[72], T. Maltsev[40,x], H. Malygina[14], G. Manca[24,f],
G. Mancinelli[8], D. Marangotto[23,q], J. Maratas[7,w], J.F. Marchand[6], U. Marconi[17],
C. Marin Benito[9], M. Marinangeli[45], P. Marino[45], J. Marks[14], P.J. Marshall[56], G. Martellotti[28],
M. Martinelli[44], D. Martinez Santos[43], F. Martinez Vidal[76], A. Massafferri[1], M. Materok[11],
R. Matev[44], A. Mathad[52], Z. Mathe[44], C. Matteuzzi[22], A. Mauri[46], E. Maurice[9,b], B. Maurin[45],
M. McCann[57,44], A. McNab[58], R. McNulty[15], J.V. Mead[56], B. Meadows[61], C. Meaux[8],
N. Meinert[70], D. Melnychuk[33], M. Merk[29], A. Merli[23,q], E. Michielin[25], D.A. Milanes[69],
E. Millard[52], M.-N. Minard[6], L. Minzoni[18,g], D.S. Mitzel[14], A. Mödden[12], A. Mogini[10],
R.D. Moise[57], T. Mombächer[12], I.A. Monroy[69], S. Monteil[7], M. Morandin[25], G. Morello[20],
M.J. Morello[26,t], O. Morgunova[72], J. Moron[32], A.B. Morris[8], R. Mountain[63], F. Muheim[54],
M. Mukherjee[68], M. Mulder[29], D. Müller[44], J. Müller[12], K. Müller[46], V. Müller[12],
C.H. Murphy[59], D. Murray[58], P. Naik[50], T. Nakada[45], R. Nandakumar[53], A. Nandi[59],
T. Nanut[45], I. Nasteva[2], M. Needham[54], N. Neri[23,q], S. Neubert[14], N. Neufeld[44],
R. Newcombe[57], T.D. Nguyen[45], C. Nguyen-Mau[45,n], S. Nieswand[11], R. Niet[12], N. Nikitin[37],
A. Nogay[72], N.S. Nolte[44], A. Oblakowska-Mucha[32], V. Obraztsov[41], S. Ogilvy[55],
D.P. O'Hanlon[17], R. Oldeman[24,f], C.J.G. Onderwater[71], A. Ossowska[31],
J.M. Otalora Goicochea[2], T. Ovsiannikova[36], P. Owen[46], A. Oyanguren[76], P.R. Pais[45],
T. Pajero[26,t], A. Palano[16], M. Palutan[20], G. Panshin[75], A. Papanestis[53], M. Pappagallo[54],
L.L. Pappalardo[18,g], W. Parker[62], C. Parkes[58,44], G. Passaleva[19,44], A. Pastore[16], M. Patel[57],
C. Patrignani[17,e], A. Pearce[44], A. Pellegrino[29], G. Penso[28], M. Pepe Altarelli[44], S. Perazzini[44],
D. Pereima[36], P. Perret[7], L. Pescatore[45], K. Petridis[50], A. Petrolini[21,h], A. Petrov[72],
S. Petrucci[54], M. Petruzzo[23,q], B. Pietrzyk[6], G. Pietrzyk[45], M. Pikies[31], M. Pili[59], D. Pinci[28],
J. Pinzino[44], F. Pisani[44], A. Piucci[14], V. Placinta[34], S. Playfer[54], J. Plews[49], M. Plo Casasus[43],
F. Polci[10], M. Poli Lener[20], A. Poluektov[8], N. Polukhina[73,c], I. Polyakov[63], E. Polycarpo[2],

14

G.J. Pomery[50], S. Ponce[44], A. Popov[41], D. Popov[49,13], S. Poslavskii[41], E. Price[50],
J. Prisciandaro[43], C. Prouve[43], V. Pugatch[48], A. Puig Navarro[46], H. Pullen[59], G. Punzi[26,p],
W. Qian[4], J. Qin[4], R. Quagliani[10], B. Quintana[7], N.V. Raab[15], B. Rachwal[32],
J.H. Rademacker[50], M. Rama[26], M. Ramos Pernas[43], M.S. Rangel[2], F. Ratnikov[39,74],
G. Raven[30], M. Ravonel Salzgeber[44], M. Reboud[6], F. Redi[45], S. Reichert[12], F. Reiss[10],
C. Remon Alepuz[76], Z. Ren[3], V. Renaudin[59], S. Ricciardi[53], S. Richards[50], K. Rinnert[56],
P. Robbe[9], A. Robert[10], A.B. Rodrigues[45], E. Rodrigues[61], J.A. Rodriguez Lopez[69],
M. Roehrken[44], S. Roiser[44], A. Rollings[59], V. Romanovskiy[41], A. Romero Vidal[43], J.D. Roth[77],
M. Rotondo[20], M.S. Rudolph[63], T. Ruf[44], J. Ruiz Vidal[76], J.J. Saborido Silva[43], N. Sagidova[35],
B. Saitta[24,f], V. Salustino Guimaraes[65], C. Sanchez Gras[29], C. Sanchez Mayordomo[76],
B. Sanmartin Sedes[43], R. Santacesaria[28], C. Santamarina Rios[43], M. Santimaria[20,44],
E. Santovetti[27,j], G. Sarpis[58], A. Sarti[20,k], C. Satriano[28,s], A. Satta[27], M. Saur[4], D. Savrina[36,37],
S. Schael[11], M. Schellenberg[12], M. Schiller[55], H. Schindler[44], M. Schmelling[13], T. Schmelzer[12],
B. Schmidt[44], O. Schneider[45], A. Schopper[44], H.F. Schreiner[61], M. Schubiger[45], S. Schulte[45],
M.H. Schune[9], R. Schwemmer[44], B. Sciascia[20], A. Sciubba[28,k], A. Semennikov[36],
E.S. Sepulveda[10], A. Sergi[49], N. Serra[46], J. Serrano[8], L. Sestini[25], A. Seuthe[12], P. Seyfert[44],
M. Shapkin[41], Y. Shcheglov[35,†], T. Shears[56], L. Shekhtman[40,x], V. Shevchenko[72], E. Shmanin[73],
B.G. Siddi[18], R. Silva Coutinho[46], L. Silva de Oliveira[2], G. Simi[25,o], S. Simone[16,d], I. Skiba[18],
N. Skidmore[14], T. Skwarnicki[63], M.W. Slater[49], J.G. Smeaton[51], E. Smith[11], I.T. Smith[54],
M. Smith[57], M. Soares[17], l. Soares Lavra[1], M.D. Sokoloff[61], F.J.P. Soler[55], B. Souza De Paula[2],
B. Spaan[12], E. Spadaro Norella[23,q], P. Spradlin[55], F. Stagni[44], M. Stahl[14], S. Stahl[44],
P. Stefko[45], S. Stefkova[57], O. Steinkamp[46], S. Stemmle[14], O. Stenyakin[41], M. Stepanova[35],
H. Stevens[12], A. Stocchi[9], S. Stone[63], B. Storaci[46], S. Stracka[26], M.E. Stramaglia[45],
M. Straticiuc[34], U. Straumann[46], S. Strokov[75], J. Sun[3], L. Sun[67], Y. Sun[62], K. Swientek[32],
A. Szabelski[33], T. Szumlak[32], M. Szymanski[4], Z. Tang[3], T. Tekampe[12], G. Tellarini[18],
F. Teubert[44], E. Thomas[44], M.J. Tilley[57], V. Tisserand[7], S. T'Jampens[6], M. Tobin[32], S. Tolk[44],
L. Tomassetti[18,g], D. Tonelli[26], D.Y. Tou[10], R. Tourinho Jadallah Aoude[1], E. Tournefier[6],
M. Traill[55], M.T. Tran[45], A. Trisovic[51], A. Tsaregorodtsev[8], G. Tuci[26,p], A. Tully[51],
N. Tuning[29,44], A. Ukleja[33], A. Usachov[9], A. Ustyuzhanin[39,74], U. Uwer[14], A. Vagner[75],
V. Vagnoni[17], A. Valassi[44], S. Valat[44], G. Valenti[17], M. van Beuzekom[29], E. van Herwijnen[44],
J. van Tilburg[29], M. van Veghel[29], R. Vazquez Gomez[44], P. Vazquez Regueiro[43],
C. Vázquez Sierra[29], S. Vecchi[18], J.J. Velthuis[50], M. Veltri[19,r], G. Veneziano[59],
A. Venkateswaran[63], M. Vernet[7], M. Veronesi[29], M. Vesterinen[52], J.V. Viana Barbosa[44],
D. Vieira[4], M. Vieites Diaz[43], H. Viemann[70], X. Vilasis-Cardona[42,m], A. Vitkovskiy[29],
M. Vitti[51], V. Volkov[37], A. Vollhardt[46], D. Vom Bruch[10], B. Voneki[44], A. Vorobyev[35],
V. Vorobyev[40,x], N. Voropaev[35], R. Waldi[70], J. Walsh[26], J. Wang[5], M. Wang[3], Y. Wang[68],
Z. Wang[46], D.R. Ward[51], H.M. Wark[56], N.K. Watson[49], D. Websdale[57], A. Weiden[46],
C. Weisser[60], M. Whitehead[11], G. Wilkinson[59], M. Wilkinson[63], I. Williams[51], M. Williams[60],
M.R.J. Williams[58], T. Williams[49], F.F. Wilson[53], M. Winn[9], W. Wislicki[33], M. Witek[31],
G. Wormser[9], S.A. Wotton[51], K. Wyllie[44], D. Xiao[68], Y. Xie[68], A. Xu[3], M. Xu[68], Q. Xu[4],
Z. Xu[6], Z. Xu[3], Z. Yang[3], Z. Yang[62], Y. Yao[63], L.E. Yeomans[56], H. Yin[68], J. Yu[68,aa],
X. Yuan[63], O. Yushchenko[41], K.A. Zarebski[49], M. Zavertyaev[13,c], D. Zhang[68], L. Zhang[3],
W.C. Zhang[3,z], Y. Zhang[44], A. Zhelezov[14], Y. Zheng[4], X. Zhu[3], V. Zhukov[11,37],
J.B. Zonneveld[54], S. Zucchelli[17,e].

[1]Centro Brasileiro de Pesquisas Físicas (CBPF), Rio de Janeiro, Brazil
[2]Universidade Federal do Rio de Janeiro (UFRJ), Rio de Janeiro, Brazil
[3]Center for High Energy Physics, Tsinghua University, Beijing, China
[4]University of Chinese Academy of Sciences, Beijing, China
[5]Institute Of High Energy Physics (ihep), Beijing, China
[6]Univ. Grenoble Alpes, Univ. Savoie Mont Blanc, CNRS, IN2P3-LAPP, Annecy, France

[7]Université Clermont Auvergne, CNRS/IN2P3, LPC, Clermont-Ferrand, France

[8]Aix Marseille Univ, CNRS/IN2P3, CPPM, Marseille, France

[9]LAL, Univ. Paris-Sud, CNRS/IN2P3, Université Paris-Saclay, Orsay, France

[10]LPNHE, Sorbonne Université, Paris Diderot Sorbonne Paris Cité, CNRS/IN2P3, Paris, France

[11]I. Physikalisches Institut, RWTH Aachen University, Aachen, Germany

[12]Fakultät Physik, Technische Universität Dortmund, Dortmund, Germany

[13]Max-Planck-Institut für Kernphysik (MPIK), Heidelberg, Germany

[14]Physikalisches Institut, Ruprecht-Karls-Universität Heidelberg, Heidelberg, Germany

[15]School of Physics, University College Dublin, Dublin, Ireland

[16]INFN Sezione di Bari, Bari, Italy

[17]INFN Sezione di Bologna, Bologna, Italy

[18]INFN Sezione di Ferrara, Ferrara, Italy

[19]INFN Sezione di Firenze, Firenze, Italy

[20]INFN Laboratori Nazionali di Frascati, Frascati, Italy

[21]INFN Sezione di Genova, Genova, Italy

[22]INFN Sezione di Milano-Bicocca, Milano, Italy

[23]INFN Sezione di Milano, Milano, Italy

[24]INFN Sezione di Cagliari, Monserrato, Italy

[25]INFN Sezione di Padova, Padova, Italy

[26]INFN Sezione di Pisa, Pisa, Italy

[27]INFN Sezione di Roma Tor Vergata, Roma, Italy

[28]INFN Sezione di Roma La Sapienza, Roma, Italy

[29]Nikhef National Institute for Subatomic Physics, Amsterdam, Netherlands

[30]Nikhef National Institute for Subatomic Physics and VU University Amsterdam, Amsterdam, Netherlands

[31]Henryk Niewodniczanski Institute of Nuclear Physics Polish Academy of Sciences, Kraków, Poland

[32]AGH - University of Science and Technology, Faculty of Physics and Applied Computer Science, Kraków, Poland

[33]National Center for Nuclear Research (NCBJ), Warsaw, Poland

[34]Horia Hulubei National Institute of Physics and Nuclear Engineering, Bucharest-Magurele, Romania

[35]Petersburg Nuclear Physics Institute (PNPI), Gatchina, Russia

[36]Institute of Theoretical and Experimental Physics (ITEP), Moscow, Russia

[37]Institute of Nuclear Physics, Moscow State University (SINP MSU), Moscow, Russia

[38]Institute for Nuclear Research of the Russian Academy of Sciences (INR RAS), Moscow, Russia

[39]Yandex School of Data Analysis, Moscow, Russia

[40]Budker Institute of Nuclear Physics (SB RAS), Novosibirsk, Russia

[41]Institute for High Energy Physics (IHEP), Protvino, Russia

[42]ICCUB, Universitat de Barcelona, Barcelona, Spain

[43]Instituto Galego de Física de Altas Enerxías (IGFAE), Universidade de Santiago de Compostela, Santiago de Compostela, Spain

[44]European Organization for Nuclear Research (CERN), Geneva, Switzerland

[45]Institute of Physics, Ecole Polytechnique Fédérale de Lausanne (EPFL), Lausanne, Switzerland

[46]Physik-Institut, Universität Zürich, Zürich, Switzerland

[47]NSC Kharkiv Institute of Physics and Technology (NSC KIPT), Kharkiv, Ukraine

[48]Institute for Nuclear Research of the National Academy of Sciences (KINR), Kyiv, Ukraine

[49]University of Birmingham, Birmingham, United Kingdom

[50]H.H. Wills Physics Laboratory, University of Bristol, Bristol, United Kingdom

[51]Cavendish Laboratory, University of Cambridge, Cambridge, United Kingdom

[52]Department of Physics, University of Warwick, Coventry, United Kingdom

[53]STFC Rutherford Appleton Laboratory, Didcot, United Kingdom

[54]School of Physics and Astronomy, University of Edinburgh, Edinburgh, United Kingdom

[55]School of Physics and Astronomy, University of Glasgow, Glasgow, United Kingdom

[56]Oliver Lodge Laboratory, University of Liverpool, Liverpool, United Kingdom

[57]Imperial College London, London, United Kingdom

[58]School of Physics and Astronomy, University of Manchester, Manchester, United Kingdom

[59]Department of Physics, University of Oxford, Oxford, United Kingdom

[60] Massachusetts Institute of Technology, Cambridge, MA, United States

[61] University of Cincinnati, Cincinnati, OH, United States

[62] University of Maryland, College Park, MD, United States

[63] Syracuse University, Syracuse, NY, United States

[64] Laboratory of Mathematical and Subatomic Physics , Constantine, Algeria, associated to [2]

[65] Pontifícia Universidade Católica do Rio de Janeiro (PUC-Rio), Rio de Janeiro, Brazil, associated to [2]

[66] South China Normal University, Guangzhou, China, associated to [3]

[67] School of Physics and Technology, Wuhan University, Wuhan, China, associated to [3]

[68] Institute of Particle Physics, Central China Normal University, Wuhan, Hubei, China, associated to [3]

[69] Departamento de Fisica , Universidad Nacional de Colombia, Bogota, Colombia, associated to [10]

[70] Institut für Physik, Universität Rostock, Rostock, Germany, associated to [14]

[71] Van Swinderen Institute, University of Groningen, Groningen, Netherlands, associated to [29]

[72] National Research Centre Kurchatov Institute, Moscow, Russia, associated to [36]

[73] National University of Science and Technology "MISIS", Moscow, Russia, associated to [36]

[74] National Research University Higher School of Economics, Moscow, Russia, associated to [39]

[75] National Research Tomsk Polytechnic University, Tomsk, Russia, associated to [36]

[76] Instituto de Fisica Corpuscular, Centro Mixto Universidad de Valencia - CSIC, Valencia, Spain, associated to [42]

[77] University of Michigan, Ann Arbor, United States, associated to [63]

[78] Los Alamos National Laboratory (LANL), Los Alamos, United States, associated to [63]

[a] Universidade Federal do Triângulo Mineiro (UFTM), Uberaba-MG, Brazil

[b] Laboratoire Leprince-Ringuet, Palaiseau, France

[c] P.N. Lebedev Physical Institute, Russian Academy of Science (LPI RAS), Moscow, Russia

[d] Università di Bari, Bari, Italy

[e] Università di Bologna, Bologna, Italy

[f] Università di Cagliari, Cagliari, Italy

[g] Università di Ferrara, Ferrara, Italy

[h] Università di Genova, Genova, Italy

[i] Università di Milano Bicocca, Milano, Italy

[j] Università di Roma Tor Vergata, Roma, Italy

[k] Università di Roma La Sapienza, Roma, Italy

[l] AGH - University of Science and Technology, Faculty of Computer Science, Electronics and Telecommunications, Kraków, Poland

[m] LIFAELS, La Salle, Universitat Ramon Llull, Barcelona, Spain

[n] Hanoi University of Science, Hanoi, Vietnam

[o] Università di Padova, Padova, Italy

[p] Università di Pisa, Pisa, Italy

[q] Università degli Studi di Milano, Milano, Italy

[r] Università di Urbino, Urbino, Italy

[s] Università della Basilicata, Potenza, Italy

[t] Scuola Normale Superiore, Pisa, Italy

[u] Università di Modena e Reggio Emilia, Modena, Italy

[v] H.H. Wills Physics Laboratory, University of Bristol, Bristol, United Kingdom

[w] MSU - Iligan Institute of Technology (MSU-IIT), Iligan, Philippines

[x] Novosibirsk State University, Novosibirsk, Russia

[y] Sezione INFN di Trieste, Trieste, Italy

[z] School of Physics and Information Technology, Shaanxi Normal University (SNNU), Xi'an, China

[aa] Physics and Micro Electronic College, Hunan University, Changsha City, China

[ab] Lanzhou University, Lanzhou, China

[†] Deceased